



# Influence of initial moisture content on creep and shrinkage of concrete at constant and cyclic ambient humidity

Anna-Lena Podhajecky · Nadja Oneschkow · Bianca Kern ·  
Ludger Lohaus · Harald S. Müller · Michael Haist

Received: 5 April 2023 / Accepted: 27 September 2023 / Published online: 26 October 2023  
© The Author(s) 2023

**Abstract** Creep and shrinkage are strongly influenced by the moisture content of concrete and by the ambient humidity. The effect of the latter is currently considered in models and design codes such as the *fib* Model Code 2010 by time-average considerations, thus totally neglecting cyclic changes in ambient humidity normally observed in outdoor structures. However, the influence of the cyclic ambient humidity on the long-term deformations of concrete compared to the constant mean humidity has barely been investigated. Therefore, the developments of creep and shrinkage of a normal-strength concrete C30/37 with three initial (before testing) moisture contents at constant humidity as well as cyclic humidity were investigated. Results demonstrate that the drying shrinkage and drying creep, but also the basic creep, are higher with higher initial moisture contents at constant ambient humidity conditions. Additionally, creep strains sharply increased up to plus 60% due to cyclic humidity compared to those due to corresponding average constant humidity. The influence of cyclic ambient humidity is more pronounced for concretes with lower initial moisture contents. Those strong

deviations in the creep behaviour (compared to existing design models) may cause severe safety risks in prestressed concrete constructions. Therefore, existing creep models should be modified considering the influence of cyclic changes in humidity and the combined influence of the initial moisture content.

**Keywords** Normal-strength concrete · Creep · Shrinkage · Cyclic humidity · Constant humidity · Initial moisture content

## List of symbols

$d$ (mm)	Diameter of specimen
$f_{cm,ref}$ (MPa)	Mean reference compressive strength tested on cylinders $d/h = 60/180$ mm
$f_{cm,cyl}$ (MPa)	Mean 28-day compressive strength tested on cylinders $d/h = 150/300$ mm
$h$ (mm)	Height of the specimen
RH (%)	Relative humidity of the ambient air
$RH_{max}$ (%)	Maximum value of cyclic humidity
$RH_{mean}$ (%)	Mean value of cyclic humidity
$RH_{min}$ (%)	Minimum value of cyclic humidity
$t$ (d)	Age of concrete
$t_0$ (d)	Age of concrete at loading
$t_c$ (d)	Age of concrete at unloading

A.-L. Podhajecky · N. Oneschkow (✉) ·  
B. Kern · L. Lohaus · M. Haist  
Institute of Building Materials Science, Leibniz  
University Hannover, Hannover, Germany  
e-mail: n.oneschkow@baustoff.uni-hannover.de

H. S. Müller  
SMP Ingenieure im Bauwesen, Karlsruhe, Germany



$t_s$ (d)	Age of concrete at the start of drying
$\Delta t_{\text{cyc}}$ (d)	Duration of a period at $\text{RH}_{\text{max}}$ or $\text{RH}_{\text{min}}$ ; duration of a half humidity cycle

### Greek letters (see Figs. 1 and 4)

$\Delta \varepsilon_{i,\text{RHmax}}$ ( $\mu\text{m}/\text{m}$ )	Change in strain within $\Delta t_{\text{cyc}}$ at $\text{RH}_{\text{max}}$
$\Delta \varepsilon_{i,\text{RHmin}}$ ( $\mu\text{m}/\text{m}$ )	Change in strain within $\Delta t_{\text{cyc}}$ at $\text{RH}_{\text{min}}$
$\varepsilon_c(t)$ ( $\mu\text{m}/\text{m}$ )	Total strain under uniaxial stress at a concrete age $t$
$\varepsilon_{cc}(t, t_0)$ ( $\mu\text{m}/\text{m}$ )	Creep strain at a concrete age $t$ loaded at age $t_0$
$\varepsilon_{cd}(t, t_0, t_e)$ ( $\mu\text{m}/\text{m}$ )	Delayed elastic strain
$\varepsilon_{cd\infty}$ ( $\mu\text{m}/\text{m}$ )	Final value for the delayed elastic strain
$\varepsilon_{ci}(t_0)$ ( $\mu\text{m}/\text{m}$ )	Elastic strain
$\varepsilon_{cs}(t, t_s)$ ( $\mu\text{m}/\text{m}$ )	Shrinkage or swelling strain at concrete age $t$
$\sigma_c(t_0)$ (MPa)	Creep stress

## 1 Introduction

Concrete is subjected to pronounced creep and shrinkage deformations which must be considered in the design of the structure. Models currently used for predicting those deformations, such as *fib* Model Code 2010 [1], Eurocode 2 [2] or ACI 209R [3], have been

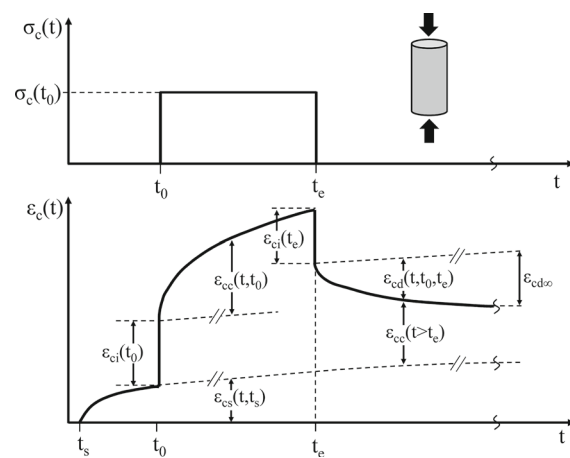


**Fig. 1** Definition of the strain components of a uniaxially loaded and unloaded concrete specimen analogous to [5] at constant climatic conditions

calibrated on laboratory creep and shrinkage tests performed under constant climatic conditions. However, it has been shown that the real deformations measured on existing reinforced and prestressed concrete bridges are significantly higher than those calculated in the design process using the previously mentioned models [4]. An underestimation of the deformations occurring in practice might lead to severe damage and safety risks. The effect of cyclic ambient humidity conditions is mentioned in the background document of *fib* Model Code 2010 [5] as a possible reason for the difference between the calculated and the measured deformations. However, this effect has barely been investigated.

The total strain  $\varepsilon_c(t)$  at constant climatic conditions due to a static creep load consists of the following strain components: the elastic strain  $\varepsilon_{ci}(t_0)$  and the time-dependent strains, such as shrinkage strain  $\varepsilon_{cs}(t, t_s)$  and creep strain  $\varepsilon_{cc}(t, t_0)$  (see Fig. 1). During the unloading of the concrete, the immediate elastic strains  $\varepsilon_{ci}(t_e)$  decrease, followed by delayed elastic strains  $\varepsilon_{cd}(t, t_0, t_e)$ , which develop over time and approach a final value  $\varepsilon_{cd\infty}$ .

The microscopic origins of creep and shrinkage strains are explained in literature as (i) sliding processes within the individual C–S–H nanoparticles or nanofoils (Feldman theory; [6]), (ii) as sliding between the aforementioned particles (Powers theory; [7]) and/or (iii) as the formation of microcracks (Wittmann theory; [8]). The microprestress-solidification theory presented by Bažant et al. [9] significantly extends this picture by taking into account eigenstresses forming in the hardened cement paste during hydration, which with increasing degree of hydration and depending on loading, might be relaxed due to the formation of slippage planes or by nano-/microcracking, thus acknowledging the established creep theories. Based on experimental investigations, Haist et al. [10] recently were able to shed new light on this long-standing scientific dispute by showing that the creep behaviour is primarily influenced by the packing density of the C–S–H nanoparticles and by a slippage occurring between these particles upon loading, thus emphasising the importance of the Powers theory. The exact role of eigenstresses, as postulated by Bažant, could not yet be quantified. However, as the C–S–H particles for typical degrees of hydration reach packing densities beyond 70 vol.% and are thus in a mechanically jammed state-i.e. translation of particles



requires dilation–shear banding must occur in the system during creep similar to soft-matter gels [11], making the presence of eigenstresses highly plausible. All of the above theories have in common that they require slippage processes to occur, which in turn are highly influenced by the presence of water. Water in the gel pores will also directly influence the packing density of the C–S–H nanoparticles, thus additionally increasing the creep deformation.

The decisive role of water on the deformation behaviour of concrete also becomes apparent from macroscopic investigations. According to *fib* Model Code 2010 [1], shrinkage and creep are divided into a basic and a drying strain component. Basic creep tests (i.e. tests performed when drying was prevented) have shown that the higher the moisture content in hardened cement paste, the higher the basic creep strain [12–14]. If concrete specimens are additionally subjected to drying, the total strains are significantly higher than for specimens remaining in a hygric equilibrium [15], resulting from drying shrinkage superimposed by drying creep processes. As a result, the total strain differs from the sum of the elastic strain, the drying shrinkage strain of the non-loaded specimen and the basic creep strain of the sealed specimen. This behaviour is called Pickett effect [16] and in the last decades various theories have been proposed trying to explain this effect. For instance, it is well accepted that the microcracking effect can explain one part of the drying creep [17, 18]. Regarding the explanation of the second part, Bažant et al. [18, 19] introduce micro-diffusion processes, which lead to a transport of water molecules between the macropores and the micropores, and this transportation promotes the breakage of bonds which leads to further creep strains. A detailed description of all theories of the mechanisms explaining drying creep is out of the scope of this paper. Driven by a higher gradient between the relative humidity (RH) of the ambient air and the moisture content of the concrete, drying shrinkage and drying creep increase with a reduction of the RH of the ambient air [15, 20] at equal initial water content. In addition, drying strains are higher for a higher initial moisture contents of the concrete [21]. It can be summarised that the significant effects of the moisture content and the RH of the ambient air on the creep and shrinkage of concrete are already comprehensively ascertained for constant ambient humidity conditions.

Concerning the influence of cyclic ambient humidity on the long-term deformations of concrete, only a few investigations are documented in literature: the results of Hansen (1960) [22] were the first published on the influence of cyclic ambient humidity on the creep and shrinkage strains. The specimens (beams with  $20 \times 50 \times 400$  mm and  $20 \times 50 \times 250$  mm) in these investigations were submerged under water and then stored for 21 days at 70% RH and 20 °C before testing. Regarding the tests at cyclic humidity, the humidity was first set to the minimum value  $RH_{\min} = 50\%$  and then changed to the maximum value  $RH_{\max} = 70\%$  after a period of 1 or 7 days. The reference tests at constant humidity were also conducted at  $RH_{\min}$  and  $RH_{\max}$  and additionally at the mean value of the cyclic humidity  $RH_{\text{mean}} = 65\%$ . Müller and Prisl [23] tested creep and shrinkage specimens (cylinders with diameter/height  $d/h = 50/200$  mm and  $d/h = 100/300$  mm) which were submerged under water before testing at a cyclic humidity between  $RH_{\max} = 90\%$  and  $RH_{\min} = 40\%$  (started with  $RH_{\max}$ ) in periods of 7 days and at constant humidity at  $RH_{\text{mean}} = 65\%$ . The ambient humidity in the investigations of Sakata et al. [24] on the influence of cyclic humidity on the creep strains was changed between  $RH_{\min} = 50\%$  and  $R_{\max} = 70\%$  in periods of 3, 5, 7, 14 and 28 days and the reference tests were conducted at a constant humidity of  $RH_{\text{mean}} = 60\%$ . No precise information was given by the authors on the storage conditions of specimens (prisms with  $100 \times 100 \times 400$  mm) other than that drying started simultaneously with loading. In the most recent investigations of Cagnon et al. (2015) [25], creep and shrinkage specimens (cylinders with  $d/h = 118/225$  mm) were stored submerged under water and then tested at a cyclic humidity between  $RH_{\min} = 50\%$  and  $RH_{\max} = 98\%$ , and at a constant humidity of  $RH_{\min} = 50\%$  as reference. Al Alusi et al. [26] also conducted creep and shrinkage tests at constant and cyclic humidity on hollow cylindrical specimens ( $h = 1016$  mm; inner diameter = 127 mm; outer diameter = 152.4 mm).

Regarding the shrinkage strains, Hansen [22] showed that the resulting strains due to cyclic humidity ( $RH_{\min}/RH_{\max}$ ) varied evenly around the strains due to constant humidity at  $RH_{\text{mean}}$ , so that the mean value of the cyclic strain curve is approximately equal to the constant curve. In contradiction, the investigations of Müller and Prisl [23] showed that the shrinkage strains due to cyclic humidity were



permanently below the strains due to constant humidity at  $RH_{\text{mean}}$ . Müller and Pristl [23] argued that these systematic differences might be related to the fact that the first period of the humidity cycle was started with  $RH_{\text{max}}$ , whereas Hansen [22] started with  $RH_{\text{min}}$ . Another explanation might be the different storage conditions in [22] and [23]. Investigations of Cagnon et al. [25] indicated that the shrinkage strains due to cyclic ambient humidity are permanently below those due to constant humidity, but here at  $RH_{\text{min}}$ . However, the maximum strain value at the end of a period of  $RH_{\text{min}}$  at cyclic humidity is close to the constant curve. The same was also shown in the results on the hollow cylindrical specimens [26]. All investigations on the influence of cyclic humidity generally revealed that hygric shrinkage strains are mostly reversible, so that the shrinkage at  $RH_{\text{min}}$  is in the same range as the swelling at  $RH_{\text{max}}$ , with the exception of irreversible strains due to the first dryings.

Regarding the effect of cyclic humidity on the creep strains, results obtained by Hansen [22] as well as Müller and Pristl [23] revealed that the creep strains are increased by approx. 20% due to cyclic humidity compared to constant  $RH_{\text{mean}}$  at the end of loading. Müller and Pristl [23], however, raised the question of whether creep is actually increased or/ and accelerated due to cyclic humidity, i.e. if creep is only accelerated at the beginning, but after years the same creep strains occur at constant and cyclic humidity. Results of Sakata et al. [24] showed that the creep strains of the specimens tested at cyclic humidity are in the same range compared to the specimens tested at constant  $RH_{\text{mean}}$ . Results of Hansen [22] further even indicated that the magnitude of creep strains tested at cyclic humidity corresponds more closely to the strains tested at constant  $RH_{\text{min}}$ , rather than at constant  $RH_{\text{mean}}$ . These results correspond to the results of Cagnon et al. [25], which showed no significant difference in the magnitude of creep strains between specimens tested at cyclic humidity and at constant  $RH_{\text{min}}$ . An increase in creep strains of hollow cylindrical specimens of approx. 200% due to cyclic humidity could even be determined compared to constant  $RH_{\text{min}}$  [26].

The cyclic tests of Vandewalle [27] were conducted with a climate profile measured in the natural environment, thus, not only the ambient humidity but also the temperature was varied in a cyclic manner. The same was also done by Li et al. [28], however, the

specimens were additionally sprayed with water in a cyclic manner. These results will thus not be discussed in further detail in this paper because the influence of cyclic ambient humidity was not systematically examined in these investigations.

It can be concluded that there is a lack of sufficient systematic and comprehensive data concerning the influence of cyclic ambient humidity on the long-term deformations of concrete. Therefore, prediction models are based almost entirely on tests conducted at constant climatic conditions tested mainly in a standard climate [5]. Cyclic changes in ambient humidity in the design approach of *fib* Model Code 2010 [1] are only considered by using the time-average of ambient humidity ( $RH_{\text{mean}}$ ) for the calculation of drying deformations. However, a few studies indicated that deformations measured at cyclic ambient humidity are not comparable to deformations at constant  $RH_{\text{mean}}$ . Models of Bažant et al. [29, 30] cover the effect of cyclic humidity conditions by inserting a correction factor into the drying creep at  $RH_{\text{mean}}$ . The correction factor considers information about the duration of the humidity period, the amplitude of the humidity variation and the cross-section thickness of the structural element. Also Torrenti et al. [31] provided a model that links the drying shrinkage at cyclic humidity to the water content of concrete. However, these models were validated using only a small database documented in literature.

Consequently, it is still necessary to investigate the influence of cyclic ambient humidity on the long-term strains of concrete. The overall objective is to comparatively investigate the creep and shrinkage behaviour due to cyclic ambient humidity and the corresponding constant mean humidity, following the design approach of *fib* Model Code 2010 [1]. In this paper, results of the influence of cyclic ambient humidity on the creep and shrinkage behaviour of a normal-strength concrete with three different initial moisture contents are presented.

## 2 Experimental programme

### 2.1 Concrete composition and specimens

All investigations were carried out on a normal-strength concrete C30/37 with a high water cement ratio of  $w/c = 0.7$ . This high  $w/c$ -ratio was chosen in



**Table 1** Concrete composition [32]

Component	Unit	Value
Ordinary Portland cement (CEM I 42.5 R)	(kg/m <sup>3</sup> )	290
Quartz powder (0/0.25 mm)	(kg/m <sup>3</sup> )	40
Natural river sand (quartzitic) (0/2 mm)	(kg/m <sup>3</sup> )	790
Natural river gravel (quartzitic) (2/8 mm)	(kg/m <sup>3</sup> )	966
PCE superplasticiser	(kg/m <sup>3</sup> )	1.7
Water	(kg/m <sup>3</sup> )	202
Water to cement ratio <i>w/c</i>	–	0.70

order to obtain a pronounced capillary pore system and a resulting accelerated drying creep and drying shrinkage as well as a low basic shrinkage behaviour. Further, such a high *w/c*-ratio was necessary to ensure the desired “low” strength. The composition of the concrete is given in Table 1. A more detailed description of the concrete composition and the raw materials used can be found in [32]. The specimens were cast in several batches with 28-day mean compressive strengths tested according to DIN EN 12390-3 [33] of  $f_{cm,cyl} = 31.8$  MPa (batch 2),  $f_{cm,cyl} = 31.5$  MPa (batch 3) and  $f_{cm,cyl} = 36.2$  MPa (batch 4), respectively.

The creep and shrinkage tests were conducted on cylindrical specimens with a height of  $h = 180$  mm and a diameter of  $d = 60$  mm. Polyvinyl chloride (PVC) formworks were used for the production of the specimens. The formworks were filled in two equal concrete layers and each layer was mechanically compacted using a vibrating table. The specimens were cast with a height of  $h = 230$  mm and later cut to the final height in order to prevent disturbed areas at

the ends of the specimens. After concreting, the specimens were covered with a wet cloth and polyethylene foil for one day. Thereafter, the specimens were stored at 20 °C in boxes with wet cloths to avoid drying. After five weeks, the formworks were removed and the specimens were cut to the final height of 180 mm. The upper and lower test surfaces of all specimens were plan-parallel ground and polished to achieve a uniform stress distribution during mechanical loading.

Afterwards, the specimens were conditioned in three different ways to ensure defined initial moisture contents in the concrete pores of approx. 100% RH (referred to as V100), approx. 75% RH (referred to as V75) and approx. 65% RH (referred to as V65). Specimens conditioned using scheme V100 were sealed with layers of plastic wrap and aluminium-coated butyl tape directly after polishing in order to prevent drying and stored at 20 °C until testing. In order to adjust the moisture contents V75 and V65, the drying durations at certain ambient humidities and temperatures were calculated based on diffusion calculations using Acosta’s [21] finite difference method and on this basis the conditioning schemes were determined. Regarding the conditioning schemes V75 and V65, only the test surfaces of the specimens were sealed to ensure a uniform drying over the circumferential surface. Afterwards, the V75 specimens were stored for 90 days at 20 °C and 65% RH and the V65 specimens for 90 days at 40 °C and 65% RH. After 90 days of drying, the V75 and V65 specimens were sealed entirely with plastic wrap and aluminium-coated butyl tape and then stored at 40 °C for further 40 days to achieve a uniform moisture

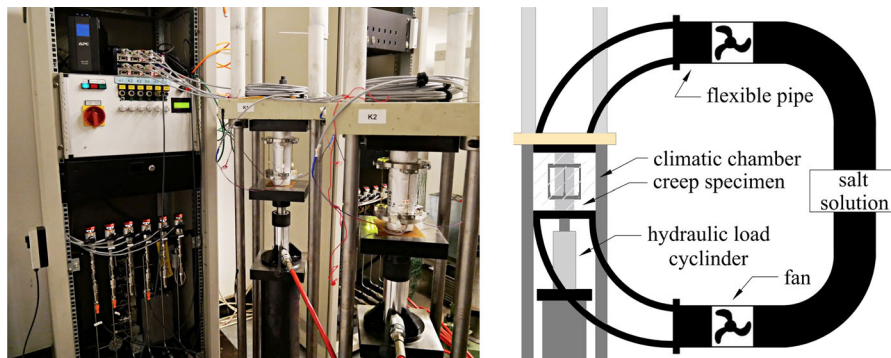


**Fig. 2** Creep testing machine (left) and schematic illustration of the climate control system for cyclic ambient humidity conditions (right)



distribution over the cross-section. Subsequently, the V75 and V65 specimens remained sealed at 20 °C until testing. As a result of the conditioning, the V75 specimens had a mass loss of approx. 22.8 g and the V65 specimens of 37.4 g. In relation to the total moisture content of the V100 specimens determined according to DIN EN ISO 12570 [34] of 57.6 g, this corresponds to a mass loss of approx. 40% and 65% for the V75 and V65 specimens, respectively.

All creep and shrinkage tests were conducted on specimens with a minimum concrete age of 180 days to ensure nearly complete hydration and to avoid additional hardening of the concrete during testing.

## 2.2 Experimental set-up

All creep tests were performed in a creep testing machine (see Fig. 2, left). The compressive force was applied with hydraulic load cylinders with a maximum load capacity of 45 kN, which were connected to a high-pressure buffer reservoir. The load precision was  $\pm 1$  kN which corresponds to  $\pm 0.4$  MPa for the specimens tested. The stress was monotonically increased up to the creep stress level within 15 s and subsequently maintained constantly until the specimens were unloaded. Shrinkage specimens were stored unloaded in the same climatic conditions.

All creep and shrinkage tests were conducted in a climate room in standard climate ( $20 \pm 1$  °C and  $65 \pm 5\%$  RH). The existing creep testing machines were modified for the tests at cyclic ambient humidity conditions (see Fig. 2, right). A climatic chamber was constructed around each creep and shrinkage specimen, connected by a pipe system to a container of saturated salt solution. The ambient humidity in the climatic chamber was adjusted to a constant target value using saturated salt solutions and two integrated fans. Cyclic ambient humidity was achieved by a cyclic change of the salt solutions potassium nitrate

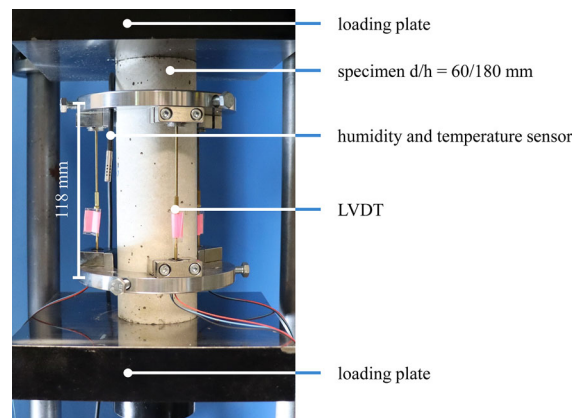


**Fig. 3** Experimental set-up without a climatic chamber

and magnesium chloride. By using these salt solutions, the ambient humidity was adjusted to  $RH_{\max} = 90 \pm 5\%$  and  $RH_{\min} = 40 \pm 5\%$  in the climatic chamber. The temperature in the climatic chamber was constant at  $22 \pm 1$  °C and, thus, slightly increased compared to the surrounding climate. In order to accelerate the changes between the ambient humidities, another container with silica gel for the dehumidification process ( $RH_{\max} \rightarrow RH_{\min}$ ) and a container with a connection to an air humidifier for the humidification process ( $RH_{\min} \rightarrow RH_{\max}$ ) was applied. Utilising this set-up, the changes between the ambient humidities were completed within approx. 2 min. Each humidity cycle was started with  $RH_{\max}$ . One humidity cycle was defined as a period of 14 days at  $RH_{\max}$  followed by 14 days at  $RH_{\min}$ , thus, 28 days in total.

The axial deformations of the specimens were measured continuously during the tests using three linear variable differential transformers (LVDTs). The LVDTs were positioned on the circumference of the specimen's axis at angles of 0°, 120° and 240°, respectively (see Fig. 3). In addition, calibrated oil pressure sensors were used to determine the axial force

**Table 2** Reference compressive strengths of cylindrical specimens at the age of loading

Initial moisture content	Reference compressive strength $f_{cm,ref}$	Concrete batch	Age of loading
V100	43.0 (MPa)	Batch 2	629 (d)
V100	46.6 (MPa)	Batch 2	818 (d)
V65	38.0 (MPa)	Batch 3	812 (d)
V75	44.3 (MPa)	Batch 4	545 (d)

acting on the specimen. The RH and the temperature of the ambient air around the specimens were measured with a calibrated capacitive humidity and temperature sensor from Driesen + Kern (RFTXXS-325). The axial force and deformations were recorded with a sampling rate of 1 Hz and the RH and temperature with a rate of 0.1 Hz.

### 2.3 Test programme

The compressive reference strength of the concrete was determined force-controlled immediately before the creep and shrinkage tests. Three specimens ( $d = 60$  mm;  $h = 180$  mm) of initial moisture contents V100, V75 and V65 were tested, respectively. The reference strengths were calculated as the mean values of the three specimens. The applied creep stress was chosen to be 35% of the reference strength.

The reference compressive strengths are summarised in Table 2. Due to the number of test specimens required for this complex test programme, the specimens had to be cast in several batches. The creep and shrinkage tests for V100 had to be divided into two experimental blocks due to limited testing capacities, whereas tests on specimens of the initial moisture contents V75 and V65, respectively, were conducted in one experimental block. The reference compressive strength of the V100 specimens increases from 629 to 818 days. However, from a statistical point of view (ANOVA, probability value  $p$ -value  $> 0.05$ ), the increase in compressive strength is not significant.

The test programme for the creep and shrinkage tests is given in Table 3 regarding the humidity conditions during the tests and the initial moisture contents of the specimens. Three humidity conditions during the tests were investigated: sealed specimens (lines 1 and 2) were tested where drying was prevented

using an aluminium-coated butyl tape. The basic creep and basic shrinkage strains were determined from these specimens. In addition, specimens were tested at a standard climate with a constant RH of 65% (lines 3 and 4) in order to calibrate the tests with available prediction models. These specimens were used to determine the drying creep and drying shrinkage strains. In order to investigate the influence of cyclic ambient humidity, specimens were tested at a cyclic ambient humidity between  $RH_{\max} = 90\%$  and  $RH_{\min} = 40\%$  (lines 5 and 6). The cyclic humidity values were chosen to cover realistic changes in the ambient humidity in Western Europe [35] and correspond on average to the constant humidity value ( $RH_{\text{mean}} = 65\%$ ). For the determination of the effect of the initial moisture content on the long-term deformations all tests were conducted on specimens with the initial moisture contents V100, V75 and V65.

The duration of all tests was 98 days, whereby the creep specimens were loaded for 91 days and subsequently unloaded with continuous strain measurement for another 7 days. The drying of the creep and shrinkage specimens was started simultaneously.

### 2.4 Data analysis

The axial deformations measured were averaged over the three axes (mean value) and then related to the measuring length of 118 mm to calculate the strains. The strains given were the mean values of two specimens (except for Table 3, line 1, V100). The total strains  $\varepsilon_c$  correspond to the strains during the creep tests. The creep strains  $\varepsilon_{cc}$  were calculated from the total strains  $\varepsilon_c$  by subtracting the elastic strains  $\varepsilon_{ci}$  and the shrinkage strains  $\varepsilon_{cs}$  from the specimens tested at the same humidity conditions. The elastic strain  $\varepsilon_{ci}$  was defined as the strain at the time when the final creep load was reached.

**Table 3** Overview of the creep and shrinkage tests conducted

Line	Load type	Humidity conditions during the tests	Number of specimens		
			V100	V75	V65
1	Creep	Sealed	1	2	2
2	Shrinkage	Sealed	2	2	2
3	Creep	Constant 65% RH	2	2	2
4	Shrinkage	Constant 65% RH	2	2	2
5	Creep	Cyclic 90/40% RH	2	2	2
6	Shrinkage	Cyclic 90/40% RH	2	2	2

The terms minimum strain value and maximum strain value were used in the following to describe the cyclic strain response. The minimum strain value is defined as the strain at the end of a half humidity cycle after a period at  $RH_{max}$  and the maximum strain value at the end of a humidity cycle after a period at  $RH_{min}$  (see Fig. 4).

The changes in strain within each period of 14 days at  $RH_{max}$ , respectively at  $RH_{min}$ , were calculated ( $\Delta\epsilon_{i,RHmax}$ ;  $\Delta\epsilon_{i,RHmin}$ ) for a further characterisation of the strains at cyclic ambient humidity. The changes in strain were calculated for each period (at  $RH_{max}$  or  $RH_{min}$ ) by subtracting the strain value at the start of the

respective period from the corresponding strain value at the end of the period. The periods of  $RH_{max}$  and  $RH_{min}$  were considered separately for the calculation and presentation of the results. In order to compare the changes in creep strain at cyclic humidity with those at constant humidity and sealed condition, the changes in creep strain of the constant and sealed tests were calculated and presented analogously for the same periods.

### 3 Results and discussion

#### 3.1 Influence of cyclic ambient humidity on the shrinkage strain

The shrinkage strains of the specimens tested at sealed conditions (red), tested at constant humidity (orange) and cyclic ambient humidity (blue) are shown in Fig. 5. In addition, the corresponding humidity conditions during the tests are shown. The shrinkage strains of specimens with an initial moisture content of approx. 100% (V100), approx. 75% (V75) and approx. 65% (V65) are presented in Fig. 5a, b and c, respectively.

It can be seen from Fig. 5 that the shrinkage strains of the specimens tested at sealed conditions and constant humidity increase with increasing test

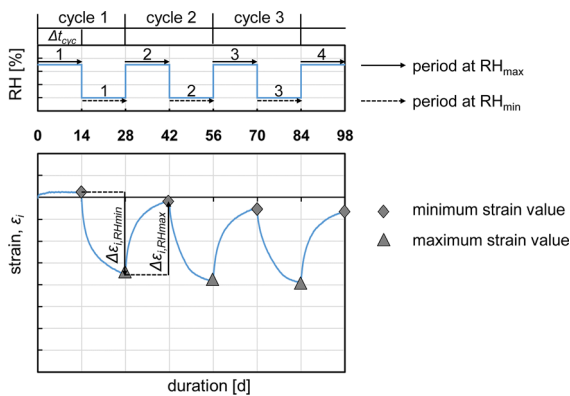


Fig. 4 Definition of the cyclic terms

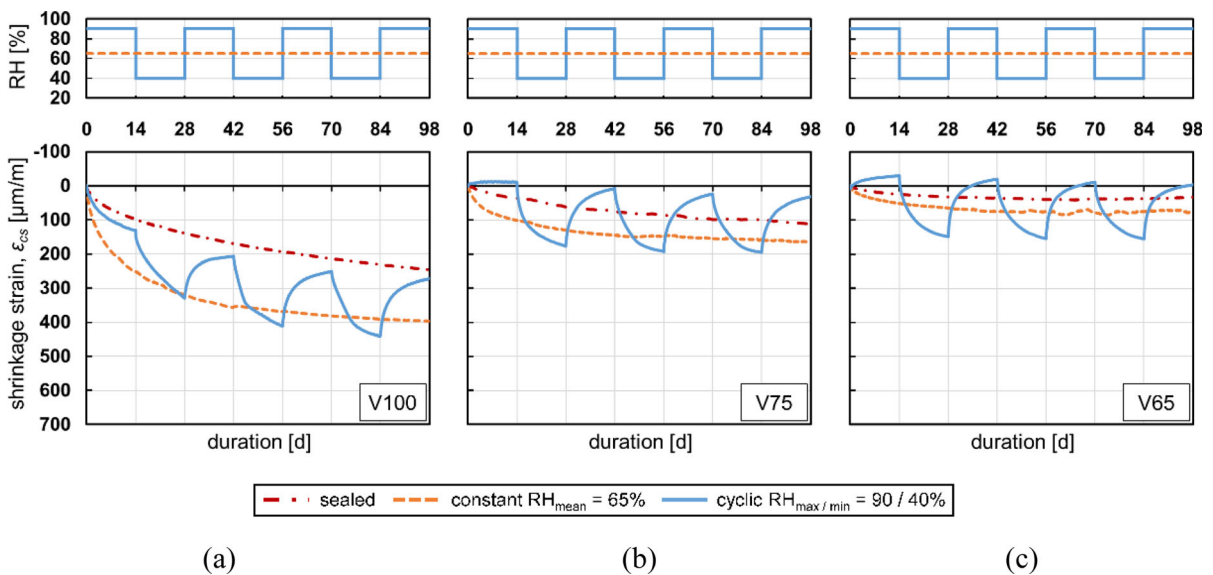


Fig. 5 Developments of shrinkage strain with initial moisture contents of approx. 100% (V100), approx. 75% (V75) and approx. 65% (V65)





duration for all initial moisture contents, which is generally expected in shrinkage tests. The shrinkage strains of specimens tested at constant humidity are higher than those of the sealed specimens (basic shrinkage). The difference between these curves generally corresponds to the drying shrinkage. However, comparing Figs. 5a, b and c, it can be seen that higher basic shrinkage strains occur with higher initial moisture contents, which was not expected for specimens with high concrete ages and  $w/c$ -ratios of 0.7. Gravimetric measurements on the sealed specimens indicate that these exhibited a mass loss during the tests despite the sealing. The V100 specimens tested sealed had a loss of moisture of approx. 9 g, which, as a reference, corresponds to about half of the mass loss of the specimens tested at constant ambient humidity. Therefore, the measured deformations include a combination of basic and drying shrinkage and no comparison is thus made in the following. However, the shrinkage strains of the sealed specimens are shown for completeness for the calculation of the creep strains. Nevertheless, it is apparent from Fig. 5 that the drying shrinkage increases with higher initial moisture contents (orange curves). This is in accordance with observations by Acosta [21].

The shrinkage strain curves of the specimens tested at cyclic ambient humidity are characterised by a cyclic strain response which shows consecutive

shrinkage and swelling. Depending on the moisture content of the specimens in relation to the ambient humidity, the specimens lose moisture and shrink or absorb moisture from the ambient air and swell. As described in sect. 2.2, the first humidity cycle was started at  $RH_{max} = 90\%$  for 14 days and then changed to  $RH_{min} = 40\%$  for 14 days. In the first period at  $RH_{max}$ , the V100 specimens (Fig. 5a) shrink due to a higher initial moisture content compared to the ambient humidity. By contrast, the V75 (Fig. 5b) and V65 specimens (Fig. 5c) swell due to a lower initial moisture content. After the first change to  $RH_{min}$ , the V100, V75 and V65 specimens shrink. Within each further humidity cycle, all specimens swell at  $RH_{max}$  and shrink at  $RH_{min}$ . It is apparent from Fig. 5 that the increase in the minimum and maximum strain values from humidity cycle to humidity cycle is higher for higher initial moisture contents.

Comparing the shrinkage strains of specimens tested at constant humidity with those tested at cyclic humidity in Fig. 5, differences can be observed, displaying a pronounced influence of the initial moisture content of the specimen. Considering the V65 specimens (Fig. 5c), it is apparent that the minimum and maximum strain values of the cyclic curve in mean correspond to the curve at constant humidity. These results are in good agreement with the results of Hansen [22]. By contrast, the maximum

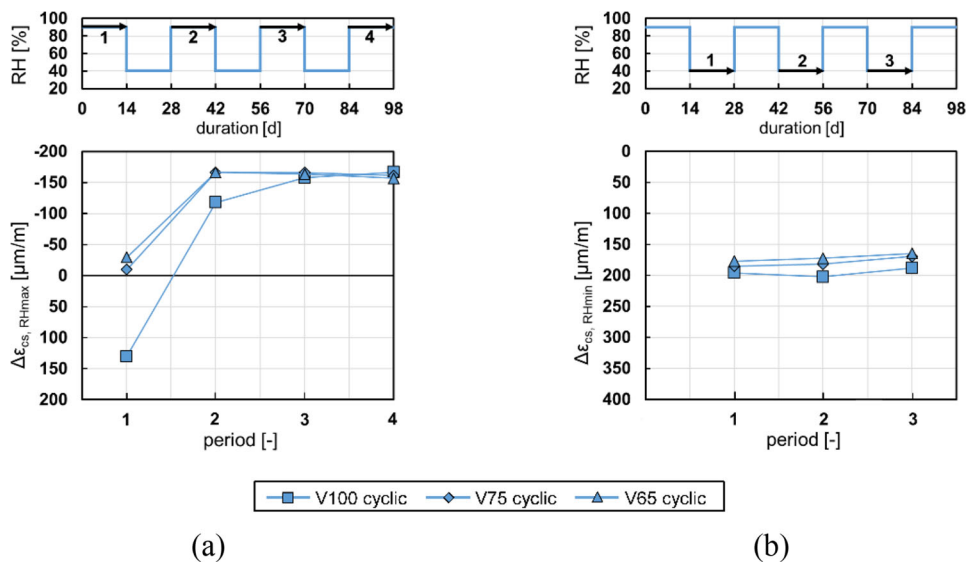


**Fig. 6** Changes in shrinkage strain within each period at  $RH_{max}$  (a) and  $RH_{min}$  (b) for the different initial moisture contents V100, V75 and V65

strain values of the cyclic curve of the V100 specimens (Fig. 5a) are closer to the constant curve than the minimum strain values. However, Müller and Pristl [23] showed that even the maximum strain values are lower than the constant curve. This may be due to a higher initial moisture content of the specimens or the shorter drying period of 7 days in the investigations of Müller and Pristl [23].

The changes in shrinkage strain within each period at  $RH_{max}$  are presented comparatively for the three initial moisture contents in Fig. 6a, and those within each period at  $RH_{min}$  are shown in Fig. 6b. When considering the changes in shrinkage strain, it is important to notice that a positive strain value is defined as shrinkage and a negative value as swelling.

Considering Fig. 6a, it is remarkable that the changes in shrinkage strain at  $RH_{max}$  converge from period to period for all three initial moisture contents. The changes in shrinkage strain from the third to the fourth period are constant and in the same range for the three initial moisture contents. It is shown in Fig. 6b that the changes in shrinkage strain at  $RH_{min}$  are nearly constant over the three humidity cycles and in the same range for the V100, V75 and V65 specimens. However, only slight differences are observed between the three initial moisture contents, whereby the V100 specimens show the highest values. Comparing Figs. 6a and b, it is apparent that the swelling at

$RH_{max}$  in the third and fourth period is almost the same as the shrinkage at  $RH_{min}$  in the third period, which indicates that the shrinkage strains are mostly reversible after the third humidity cycle.

In total, the results of Figs. 5 and 6 show that the relation between the shrinkage strains due to cyclic humidity and constant humidity at  $RH_{mean}$  depends on the initial moisture content of the concrete. However, the results further indicate that the changes in shrinkage strain of the three initial moisture contents converge, so it can be assumed that the moisture contents in the specimens also converge. This needs to be confirmed in further investigations on measurements of the internal RH of concrete during the shrinkage tests.

### 3.2 Influence of cyclic ambient humidity on the total strain

The total strains of specimens tested at sealed conditions (red), at constant humidity (orange) and cyclic ambient humidity (blue) are shown in Fig. 7 for the different initial moisture contents V100, V75 and V65, respectively. Whereas the curves represent the mean value from two tests each, for the V100 specimens tested at sealed conditions (Fig. 7 a, red), a repetition test was not possible due to limited testing capacities. However, comparable investigations from

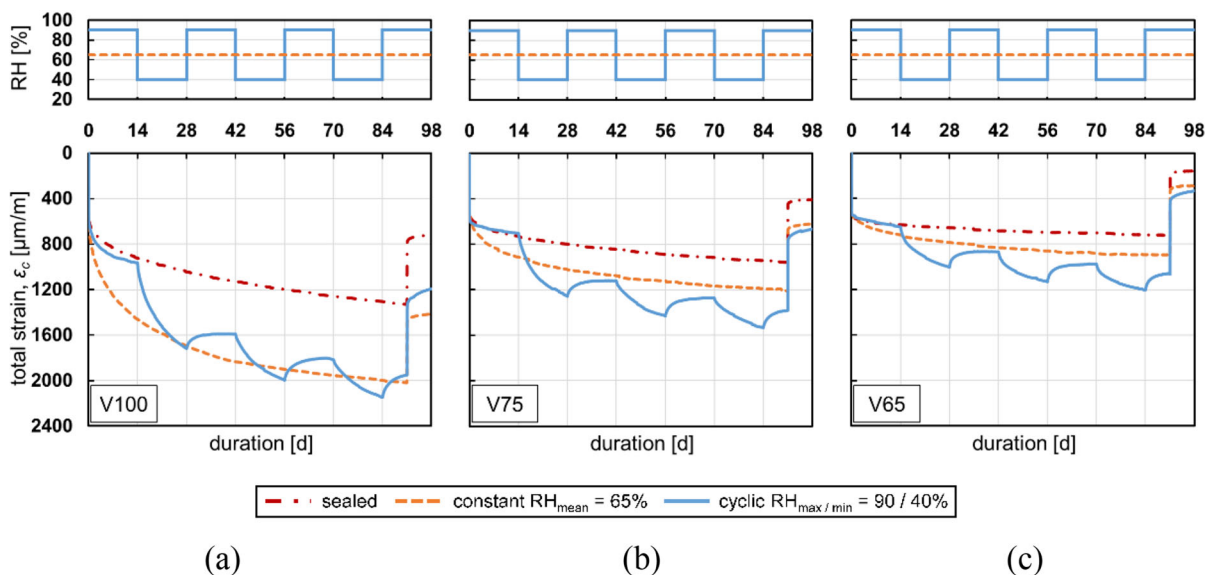


**Fig. 7** Development of total strains subjected to a degree of loading of  $0.35 f_{cm,ref}$  with initial moisture contents of approx. 100% (V100), approx. 75% (V75) and approx. 65% (V65)



a collaborative project tested on another concrete batch of the same concrete composition and initial moisture content showed similar strain developments [36].

It can be seen in Fig. 7 that the total strains of the specimens tested at sealed conditions and constant humidity show the expected strain components, as presented in Fig. 1. Comparing Fig. 7a, b and c, it can be seen that the elastic strains at the time of loading are approximately in the same range for the three initial moisture contents, therefore, due to only slight differences in the strains and different concrete batches, no significant influence of the initial moisture content on the elastic strains can be identified in these results. However, it is known in literature that the modulus of elasticity is higher for concretes under saturated conditions due to the incompressibility of the water in the pores [21]. It is obvious in Fig. 7 that the time-dependent strains increase with higher initial moisture contents.

Cyclic ambient humidity conditions result in a cyclic strain response even when subjected to a degree of loading of  $0.35 f_{cm,ref}$ . This demonstrates that concrete swells even under load. Similar reasoning was presented by Cagnon et al. [25]. However, swelling under load is not considered in current modelling approaches [1–3], thus requiring an adaptation of the models.

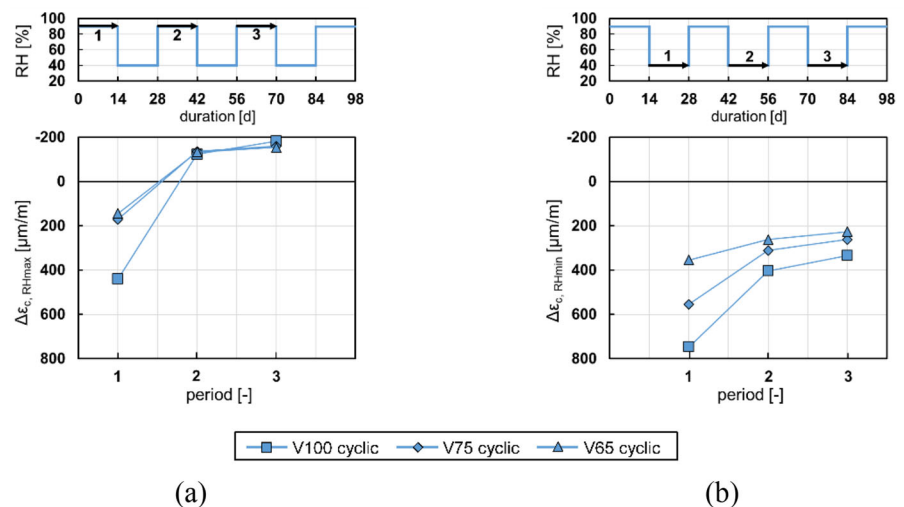
Comparing the total strains at constant  $RH_{mean}$  and cyclic humidity, it is apparent that the total strains of the V75 (Fig. 7b) and V65 specimens (Fig. 7c) tested at cyclic humidity exceed the strains observed at

constant humidity after the first humidity cycle. By contrast, the total strains of the cyclic tests of the V100 specimens (Fig. 7a) are only slightly higher than those of the constant tests at the end of the second and third humidity cycle. At the time of unloading, the elastic strains and the delayed elastic strains of the cyclic tests are higher than those of the constant tests for all initial moisture contents. Considering that the specimens at cyclic humidity were tested at  $RH_{max}$  in the last 7 days before unloading, it can be assumed that these specimens had a higher moisture content at the time of unloading compared to the specimens tested at constant humidity and, therefore, the compressed water in the concrete pores expands at the time of unloading. The specimens at cyclic humidity in the unloaded 7 days at  $RH_{max}$  probably show a swelling due to the high ambient humidity in addition to the delayed elastic strains.

The changes in total strain of the specimens at cyclic humidity within each period at  $RH_{max}$  and at  $RH_{min}$  are compared in Fig. 8 for the initial moisture contents V100, V75 and V65. The changes in total strain within each period at  $RH_{max}$  are shown in Fig. 8a and those at  $RH_{min}$  in Fig. 8b.

Comparing Figs. 6a (shrinkage strains) and 8a (total strains), the same pattern can be observed, except for the fact that the change in total strain corresponds to a reduction in length in the first period for all initial moisture contents, whereas in the shrinkage strain (see Fig. 6a) both, shrinkage as well as swelling were found, depending on the initial moisture content. Furthermore, the swelling in the

**Fig. 8** Changes in total strain within each period at  $RH_{max}$  (a) and  $RH_{min}$  (b) for the different initial moisture contents V100, V75 and V65



shrinkage strains (unloaded) is in the same range as that observed in the total strains (under load) for all initial moisture contents. Considering Fig. 8b, it becomes apparent that the changes in total strain at  $RH_{\min}$  are dependent on the initial moisture content of the specimens, so the V100 specimens show a higher change in the total strain compared to the V75 and V65 specimens. However, the changes in total strain converge over the periods for the three initial moisture contents. Comparing these results with the changes in shrinkage strain in Fig. 6b, it can be seen that the influence of the initial moisture content is increased by the mechanical load.

### 3.3 Influence of cyclic ambient humidity on the creep strain

The creep strains of specimens at sealed conditions, at constant humidity and cyclic humidity are shown in Fig. 9 for the three initial moisture contents. The colour scheme and layout are identical to Figs. 5 and 7. The shrinkage strains of the specimens tested under the same humidity conditions were subtracted from the total strains in order to calculate the creep strains. This means, in the case of the creep strains of the sealed specimens, that the (unwanted) drying shrinkage strains, which occurred despite the sealing, were subtracted, so it can be assumed that only minor drying

creep strains are included additionally to the basic creep. However, these results must be treated with care, as the magnitude of these unwanted strains is unknown. Nevertheless, comparing Figs. 9a, b and c, the results indicate that the creep strains of the sealed specimens, which correspond almost to basic creep, are higher for higher initial moisture contents. This is consistent with the results of Wittmann [12], who ascertained that specimens, where drying was prevented, show higher creep strains with higher initial moisture contents. The difference between the creep strains of the sealed specimens and those at constant humidity, which in general corresponds to the drying creep, also increases with higher initial moisture contents.

Comparing the creep strains at constant  $RH_{\text{mean}}$  and cyclic humidity, it is apparent that the first humidity cycle is decisive for the difference between these curves. At the end of the first humidity cycle, the creep strain at cyclic humidity of the V100 specimens is in the same range as that of the specimens at constant humidity, whereas the strains of the V75 and V65 specimens at cyclic humidity exceed the strains at constant humidity significantly and are, subsequently, permanently higher than the strains at constant humidity. After the second humidity cycle, the creep strain at cyclic humidity of the V100 specimens is slightly higher than at constant humidity. This

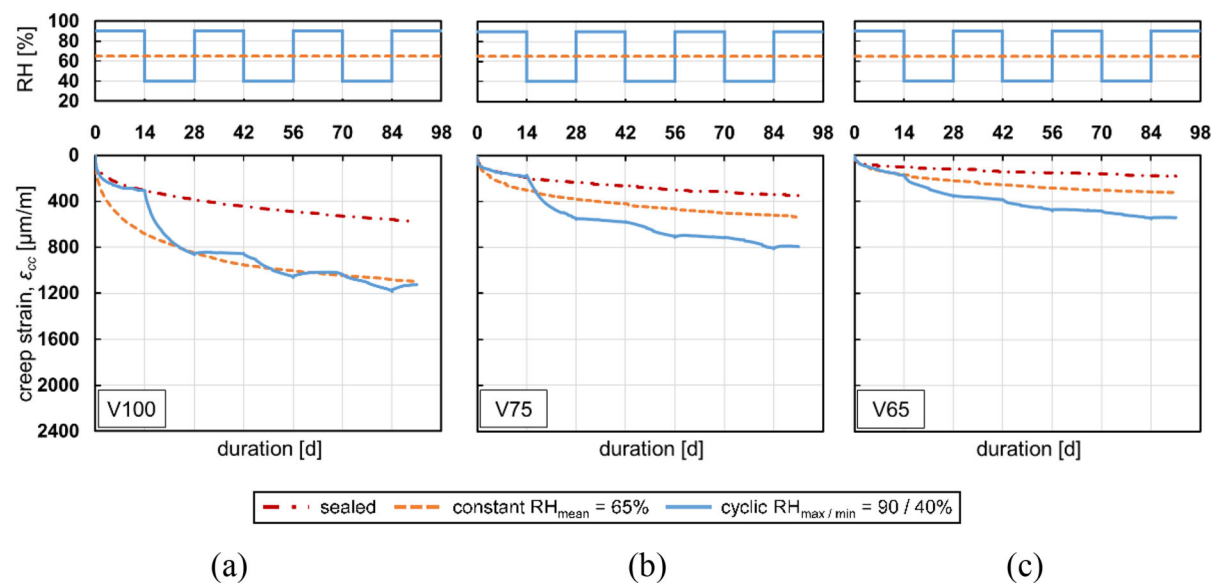


**Fig. 9** Development of creep strains subjected to a degree of loading of  $0.35 \cdot f_{\text{cm,ref}}$  with initial moisture contents of approx. 100% (V100), approx. 75% (V75) and approx. 65% (V65)



difference increases after the third humidity cycle. It can be assumed that the difference between the cyclic and constant curves of the V100 specimens will become more significant with further humidity cycles.

In summary, it can be seen that the creep strains are increased due to cyclic ambient humidity compared to those at constant  $RH_{mean}$  for all initial moisture contents. These results are in good agreement with [22, 23, 25], however, they seem to contradict with the observations by Sakata et al. [24]. In the investigations of the latter, specimens with a high initial moisture content were tested and it is evident from the results that the creep strains at cyclic humidity with a period of two weeks already slightly exceed the creep strains at constant  $RH_{mean}$  after 70 days, which is in line with the results of the V100 specimens.

Immediately before unloading, the creep strains at cyclic humidity of the V100, V75 and V65 specimens were 3, 47 and even 60% higher, respectively, compared to those subjected to the corresponding constant mean humidity. Therefore, the influence of the cyclic ambient humidity on the creep strains is higher in percentage terms for concretes with lower initial moisture contents. In addition, it is apparent that the cyclic strain response is more visible in the creep curve of the V100 specimens compared to the V75 and

V65 specimens. This needs to be investigated in further detail.

The changes in creep strain of the specimens at cyclic humidity within each period at  $RH_{max}$  and  $RH_{min}$  are compared in Fig. 10 as a function of the initial moisture content. The changes in creep strain within each period at  $RH_{max}$  are shown in Fig. 10 a and those at  $RH_{min}$  in Fig. 10 b. In addition, the changes in creep strain of the specimens at sealed conditions and constant humidity in the same periods as in the cyclic tests are detailed.

It is apparent in Fig. 10a that by subtracting the shrinkage strains from the total strains, the partial swelling observed under load of the specimens at cyclic humidity ( $RH_{max}$ ) is almost compensated in the creep strains. This indicates that the swelling under load primarily results from the shrinkage strain. In addition, it is evident that the change in creep strain at cyclic humidity is approximately the same as the change in the sealed condition, with the exception of the V65 specimens in the first period, i.e. drying creep seems to be completely stopped during the periods at  $RH_{max}$  and only basic creep continues to evolve. After the third period, there are only slight differences in the change of creep strains between the three initial moisture contents and between the three humidity

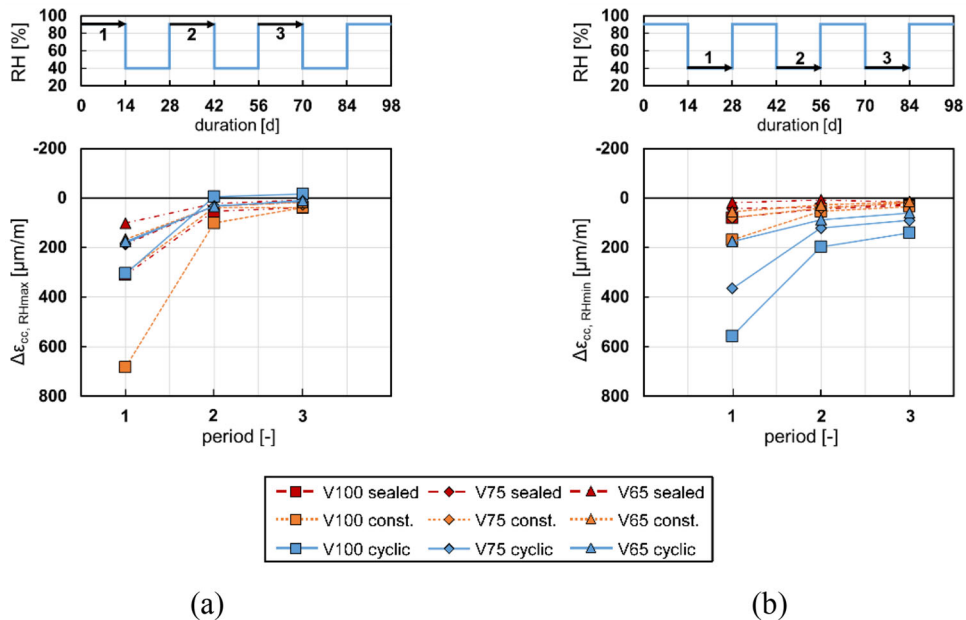


**Fig. 10** Changes in creep strain within each period at  $RH_{max}$  (a) and  $RH_{min}$  (b) for the different initial moisture contents V100, V75 and V65



conditions. Comparing Figs. 8b and 10b, it is obvious that the creep strains at cyclic humidity are shifted to lower strain values compared to the total strains. Nevertheless, the same tendencies can be observed. However, it is remarkable that the changes in creep strain in the third period of the specimens at cyclic humidity are higher than of the specimens at sealed condition and constant humidity, whereas the changes in creep strain of the specimens at sealed condition and at constant humidity are in the same range. The fact that the changes in creep strain at constant humidity in Figs. 10a and b show almost no drying creep after the third period, while the change in creep strain at cyclic humidity in Fig. 10b is still higher than those at constant humidity, indicates an increase and not only an acceleration of the creep process due to cyclic humidity compared to constant  $RH_{\text{mean}}$ .

#### 4 Conclusions and outlook

The overall objective of the research presented was to examine the influence of cyclic ambient humidity conditions on the long-term deformation behaviour of concrete and to set the basis to improve the design approaches for the calculation of these strains. The investigations presented in this paper focus on the comparison between the developments of strains due to cyclic and constant ambient humidity conditions, considering the additional influence of the initial moisture content of concrete on these strain developments. Accordingly, creep and shrinkage tests were conducted at a cyclic ambient humidity between  $RH_{\text{max}} = 90\%$  and  $RH_{\text{min}} = 40\%$  and at a constant humidity of  $RH_{\text{mean}} = 65\%$ . The constant humidity value corresponded to the time-average of the cyclic humidity, following the design approach of *fib* Model Code 2010 [1]. Within the investigations presented, a normal-strength concrete C30/37 with three initial moisture contents of approx. 100% (V100), approx. 75% (V75) and approx. 65% (V65) was tested.

The overall results obtained for different initial moisture contents of the specimens and different humidity conditions during the tests can be concluded as follows:

- The basic creep increases with higher initial moisture contents.
- Cyclic ambient humidity results in a cyclic strain response even under loading (total strains), proving that concrete swells under load. Almost no swelling occurred in the creep strains at  $RH_{\text{max}}$ , so the swelling under load results primarily from the shrinkage strain component (i.e. the swelling of the non-loaded concrete). In the periods at  $RH_{\text{max}}$ , the cyclic creep strain is about the same as the basic creep strain. Consequently, drying creep seems to be completely stopped during the periods at  $RH_{\text{max}}$  and only basic creep continues to evolve. Looking at the microstructure and following the reasoning of Bažant [9, 37], this might be interpreted as a relaxation of the inner stress state of the micro-prestressed hardened cement gel by the absorption of water in the pore system.
- The relation between the shrinkage strains due to cyclic humidity and due to constant humidity at  $RH_{\text{mean}}$  depends on the initial moisture content of the concrete. However, the results indicate that the changes in shrinkage strain of the three initial moisture contents converge with an increasing number of humidity cycles.
- Creep strains are significantly increased up to plus 60% at the end of loading due to cyclic humidity compared to creep strains at constant  $RH_{\text{mean}}$ . In addition, the influence of cyclic ambient humidity increases with a lower initial moisture content of the concrete. The analysis of the changes in creep strain at  $RH_{\text{min}}$  indicates that the cyclic humidity increases and not only accelerates the creep strains.

These results reveal that the assumption of a constant mean ambient humidity (time-average) for the calculation of creep strains in the design approach of *fib* Model Code 2010 [1] is not suitable. Variations in the ambient humidity might lead to severe damages and safety risks of deflection-sensitive structures designed with creep models, assuming a constant mean humidity  $RH_{\text{mean}}$ . The results also reveal the requirement to directly include the influence of the initial moisture content for the design of basic creep, drying creep and drying shrinkage.

Therefore, it is relevant to investigate further the influence of cyclic humidity conditions and the combined influence of the initial moisture content of concrete in more detail. Investigations into concretes with a less pronounced pore system are scheduled



within the scope of this research project. In addition, the development of the internal RH of the concrete during creep and shrinkage under cyclic and constant ambient humidity conditions will be investigated. Based on these results, an adaptation or improvement of current deformation prediction models for cyclic humidity conditions is planned.

**Acknowledgements** The authors would like to express their gratitude to the German Research Foundation (DFG) for the financial support.

**Author contributions** Conceptualisation: ALP, NO and MH; methodology: ALP, NO and MH; formal analysis and investigation: ALP and BK; writing—original draft preparation: ALP and NO; writing—review and editing: ALP, NO, BK, LL, HM and MH and funding acquisition: HM and MH. All authors agreed to the final draft of the text.

**Funding** Open Access funding enabled and organized by Projekt DEAL. This research was funded by the German Research Foundation (DFG) within the project “Creep and shrinkage at variable hygric exposures”, project number 327002599. Open Access funding enabled and organised by Projekt DEAL.

#### Declarations

**Conflict of interest** The authors have no conflicts of interest to declare that are relevant to the content of this article.

**Open Access** This article is licensed under a Creative Commons Attribution 4.0 International License, which permits use, sharing, adaptation, distribution and reproduction in any medium or format, as long as you give appropriate credit to the original author(s) and the source, provide a link to the Creative Commons licence, and indicate if changes were made. The images or other third party material in this article are included in the article’s Creative Commons licence, unless indicated otherwise in a credit line to the material. If material is not included in the article’s Creative Commons licence and your intended use is not permitted by statutory regulation or exceeds the permitted use, you will need to obtain permission directly from the copyright holder. To view a copy of this licence, visit <http://creativecommons.org/licenses/by/4.0/>.

#### References

1. *fib*—Fédération Internationale du Béton (2013) *fib* model code for concrete structures 2010. Ernst & Sohn, Berlin. <https://doi.org/10.35789/fib.BULL.0055>
2. EN 1992-1-1 (2004) Eurocode 2: Design of concrete structures—Part 1-1: General rules and rules for buildings. CEN: Brussels
3. ACI Committee 209 (1992) Prediction of creep, shrinkage and temperature effects in concrete structures (ACI 209R-92) (Reapproved 2008). American Concrete Institute, Farmington Hills
4. Bažant ZP, Yu Q, Hubler MH, Křístek V, Bittnar Z (2011) Wake up call for creep, myth about size effect and black holes in safety: What to improve in *fib* model code draft. In: Proceedings of *fib* symposium: concrete engineering for excellence and efficiency, Prague, Czech Republic, June 8–10, 2:731–746
5. *fib*—Fédération Internationale du Béton (2013) Code-type models for structural behaviour of concrete: Background of the constitutive relations and material models in the *fib* model code for concrete structures 2010; state-of-art report. *fib* bulletin no.70, Lausanne, Switzerland. <https://doi.org/10.35789/fib.BULL.0070>
6. Feldman RF (1972) Mechanism of creep of hydrated Portland cement paste. *Cem Concr Res* 2(5):521–540. [https://doi.org/10.1016/0008-8846\(72\)90107-X](https://doi.org/10.1016/0008-8846(72)90107-X)
7. Powers TC (1968) The thermodynamics of volume change and creep. *Mater Constr* 1(6):487–507. <https://doi.org/10.1007/BF02473638>
8. Wittmann FH (1982) Creep and shrinkage mechanisms. In: Bažant ZP, Wittmann FH (eds) *Creep and shrinkage in concrete structures*. John Wiley & Sons Ltd., New Jersey, pp 129–161
9. Bažant ZP, Hauggaard AB, Baweja S, Ulm F-J (1997) Microprestress-solidification theory for concrete creep. I: aging and drying effects. *J Eng Mech* 123(11):1188–1194. [https://doi.org/10.1061/\(ASCE\)0733-9399\(1997\)123:11\(1188\)](https://doi.org/10.1061/(ASCE)0733-9399(1997)123:11(1188))
10. Haist M, Divoux T, Krakowiak KJ, Skibsted J, Pellenq RJM, Müller HS, Ulm F-J (2021) Creep in reactive colloidal gels: a nanomechanical study of cement hydrates. *Phys Rev Research* 3:043127. <https://doi.org/10.15488/11784>
11. Aime S, Ramos L, Cipelletti L (2018) Microscopic dynamics and failure precursors of a gel under mechanical load. In: Proceedings of the national academy of science of the United States of America 115(14):3587–3592. <https://doi.org/10.1073/pnas.1717403115>
12. Wittmann FH (1970) Einfluss des Feuchtigkeitsgehaltes auf das Kriechen von Beton. [Influence of moisture content on creep of concrete] (in German). *Rheol Acta* 9:282–287. <https://doi.org/10.1007/BF01973489>
13. Pihlajavaara SE (1974) A review of some of the main results of a research on the ageing phenomena of concrete: effect of moisture conditions on strength, shrinkage and creep of mature concrete. *Cem Concr Res* 4(5):761–771. [https://doi.org/10.1016/0008-8846\(74\)90048-9](https://doi.org/10.1016/0008-8846(74)90048-9)
14. Torrenti JM, Boumediene N, Abudushalamu A (2023) Dependence of basic creep on the relative humidity. *fib* 2023 Symposium Istanbul, Jun 2023, Istanbul, Turkey, pp 256–256. [https://doi.org/10.1007/978-3-031-32519-9\\_23](https://doi.org/10.1007/978-3-031-32519-9_23)
15. Troxell E, Raphael JM, Davis RE (1958) Long-time creep and shrinkage tests of plain and reinforced concrete. *ASTM Proc* 58:1101–1120
16. Pickett G (1942) The effect of change in moisture content on the creep of concrete under a sustained load. *ACI J Proc* 38:333–355. <https://doi.org/10.14359/8607>
17. Wittmann FH, Roelfstra PE (1980) Total deformation of loaded drying concrete. *Cem Concr Res* 10(5):601–610. [https://doi.org/10.1016/0008-8846\(80\)90023-X](https://doi.org/10.1016/0008-8846(80)90023-X)



18. Bažant ZP, Xi Y (1994) Drying creep of concrete: constitutive model and new experiments separating its mechanisms. *Mater Struct* 27(1):3–14. <https://doi.org/10.1007/BF02472815>
19. Bažant ZP, Chern JC (1985) Concrete creep at variable humidity: constitutive law and mechanism. *Mater Struct* 18(1):1–20. <https://doi.org/10.1007/BF02473360>
20. Acker P, Ulm F-J (2001) Creep and shrinkage of concrete: physical origins and practical measurement. *Nucl Eng Des* 203(2–3):143–158. [https://doi.org/10.1016/S0029-5493\(00\)00304-6](https://doi.org/10.1016/S0029-5493(00)00304-6)
21. Acosta Urrea F (2018) Influence of elevated temperatures up to 100 °C on the mechanical properties of concrete. Dissertation, Karlsruhe Institute of Technology, KIT Scientific Publishing, vol 84. <https://doi.org/10.5445/KSP/1000082992>
22. Hansen TC (1960) Creep of concrete. The influence of variations in the humidity of the ambient atmosphere. In: Proceedings of the 6th congress of the IABSE, Stockholm, Sweden, Swedish Cement and Concrete Research Institute, 6:57–65
23. Müller HS, Pristl M (1993) Creep and shrinkage of concrete at variable ambient conditions. In: Proceedings of the 5th international RILEM symposium, Bažant ZP and Carol I, (eds), E. & F.N. SPON, London
24. Sakata K, Ayano T (2000) Effect of ambient temperature and humidity on creep and shrinkage of concrete. In: ACI Symposium Publication 194:215–235. <https://doi.org/10.14359/9894>
25. Cagnon H, Vidal T, Sellier A, Bourbon X, Camps G (2015) Drying creep in cyclic humidity conditions. *Cem Concr Compos* 76:91–97. <https://doi.org/10.1016/j.cemconres.2015.05.015>
26. Al-Alusi HR, Bertero VV, Polívka M (1978) Einflüsse der Feuchte auf Schwinden und Kriechen von Beton. [Effects of humidity on shrinkage and creep of concrete] (in German). *Beton-Stahlbetonbau* 73(1):18–23. <https://doi.org/10.1002/best.197800040>
27. Vandewalle L (2000) Concrete creep and shrinkage of cyclic ambient conditions. *Cem Concr Compos* 22:201–208. [https://doi.org/10.1016/S0958-9465\(00\)00004-4](https://doi.org/10.1016/S0958-9465(00)00004-4)
28. Li P, He S (2018) Effects of variable humidity on the creep behavior of concrete and the long-term deflection of RC beams. *Adv Civ Eng* 1-12. <https://doi.org/10.1155/2018/8301971>
29. Bažant ZP, Wang T-S (1985) Practical prediction of cyclic humidity effect in creep and shrinkage of concrete. *Mater Struct* 18(4):247–252. <https://doi.org/10.1007/BF02472911>
30. Bažant ZP, Kim J-K (1992) Improved prediction model for time-dependent deformations of concrete: part 5–cyclic load and cyclic humidity. *Mater Struct* 25(3):163–169. <https://doi.org/10.1007/BF02472430>
31. Torrenti JM, Granger L, Diruy M, Genin P (1999) Modelling concrete shrinkage under variable ambient conditions. *Mater J* 96(1):35–39. <https://doi.org/10.14359/425>
32. Kern B, Oneschkow N, Podhajecky A-L, Lohaus L, Anders S, Haist M (2021) Comparative analysis of concrete behaviour under compressive creep and cyclic loading. *Int J Fat* 15:106409. <https://doi.org/10.1016/j.ijfatigue.2021.106409>
33. DIN EN 12390-3:2019-10. Testing of hardened concrete—part 3: compressive strength of test specimens, German version of EN 12390-3:2019. <https://doi.org/10.31030/3045735>
34. DIN EN ISO 12570:2018-07. Hygrothermal performance of building materials and products—determination of moisture content by drying at elevated temperature, German version of EN ISO 12570:2000 + A1:2013 + A2:2018. <https://doi.org/10.31030/2849834>
35. New M, Lister D, Hulme M, Makin I (2002) A high-resolution data set of surface climate over global land areas. *Clim Res* 21:1–25. <https://doi.org/10.3354/CR021001>
36. Kern B, Oneschkow N, Haist M, Lohaus L (2022) Influence of moisture content on strain development of concrete subjected to compressive creep and cyclic loading. In: Zingoni A (ed) Current perspectives and new directions in mechanics, modelling and design of structural systems. Proceedings of the eighth International Conference on Structural Engineering, Mechanics and Computation, 5–7 September 2022, Cape Town, South Africa. Routledge, New York, pp 1357–1363. <https://doi.org/10.1201/9781003348443-221>
37. Bažant ZP, Prasannan S (1989) Solidification theory for concrete creep. I: formulation. *J Eng Mech* 115(8):1691–1703. [https://doi.org/10.1061/\(ASCE\)0733-9399\(1989\)115:8\(1691\)](https://doi.org/10.1061/(ASCE)0733-9399(1989)115:8(1691))

**Publisher's Note** Springer Nature remains neutral with regard to jurisdictional claims in published maps and institutional affiliations.

